Damage Localization in an Aluminum Plate Using Built-In Piezo-electric Sensor Induced Ultrasonic Signals

KAI JUN CHEN[1], GALEN JIANG[1], RUIDE "READER" WANG[1], EVAN HEDDING[1], SANJOT "SUNNY" SINGH[1], DANIEL OLUWALANA[1], JOONGHYUN LEE[1], NEILABJO MAITRA[1], ISAIAH COLOBONG[1], SAMAN FARHANGDOUST[2], SHABBIR AHMED[2] and FU-KUO CHANG[2]

ABSTRACT

This paper summarizes a study by students taking the class of AA257 Structural Health Monitoring of Spring of 2023 at Stanford University as a term project to predict the location and size of a single crack in an Aluminum plate using ultrasonic waves induced by surface-mounted piezoelectric discs as sensors or actuators. Three methods were presented for determining cracks in the structure, which include: i) calculating the ratio of the raw signals for different paths, ii) evaluating the ratio of the scattered signals for different paths, and iii) determining the damage index for different paths. Of the three methods presented, the second and the third method using the scatter and the damage index, respectively, are the most accurate in locating the crack.

INTRODUCTION

This work explores three distinct guided waves based active SHM techniques using piezoelectric (PZT) sensors on an aluminum plate as part of the AA257 Structural Health Monitoring class project. This paper presents the results of the efforts by a group of graduate students who participated in a blind test term-project to locate and quantify a crack in an aluminum plate where the sensor data were provided before and after a crack was introduced. The objective was to locate the crack if present and then estimate the size, if possible, without resorting to any existing techniques published in the literature.

Structural health monitoring refers to the process of damage diagnosis within a structure. By implementing an effective SHM system, one can both minimize down-time and reduce inspection duration, which can lead to significant cost savings for stakeholders [1-9].

1. Graduate students, Stanford University, Stanford, CA, USA.
2. Structures and Composites Lab, Aeronautics and Astronautics Department, Stanford University, Stanford, CA, USA.

PROBLEM STATEMENT AND EXPERIMENTAL SETUP

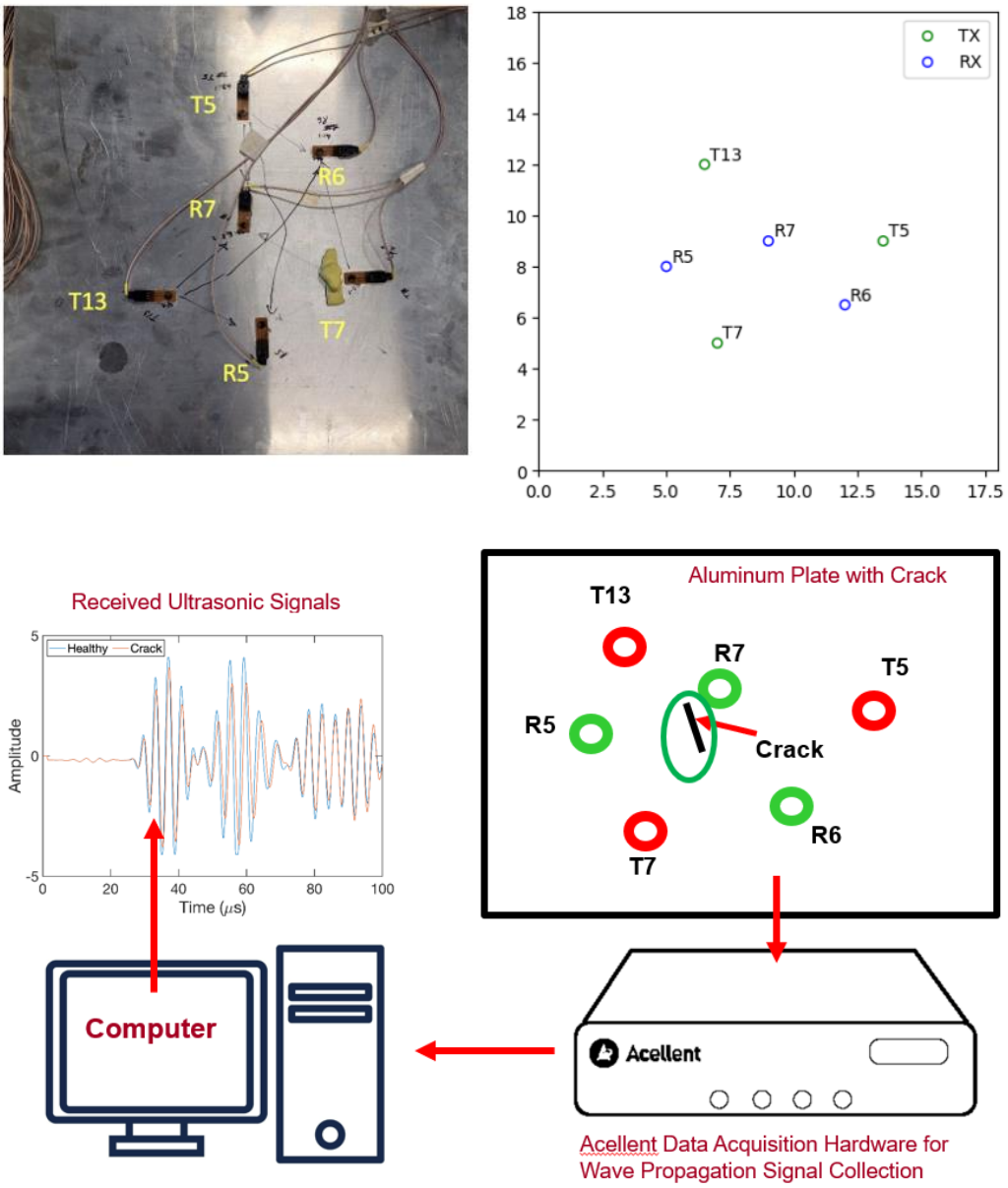

Figure 1. (top left) The aluminum plate fitted with piezoelectric sensors which was used in this study; (top right) the location of the transmitter (T) and receiver (R) on the aluminum plate; (bottom) the schematic of the complete experimental setup.

Given an 18 by 18-inch aluminum plate with six PZT sensors placed in various positions as shown in Figure 1. Three of the sensors (T5, T7, T13) are used as transmitters or actuators while the other three sensors (R5, R6, R7) are used to receive the transmitted signals. A 5-peak tone-burst actuation was used for actuating the PZT sensors. Three separate actuation frequencies, 150 kHz, 250 kHz and 350 kHz were used for exciting the PZT transducers. The setup had nine separate paths for analysis. Data were collected

using Acellent ScanSentry [9] for four different cases: one baseline without any defect, two with a sticky patch applied, and one with a hole drilled into the plate.
The sticky patch data were provided to students to calibrate the system and signals along with the baseline. The location and size of crack were kept away from the students as the blind test among the three teams formed from the class.

Table 1: The transmitter-receiver layout and frequencies used.

Path Number	Path Description	Frequencies (kHz)
1	T7 - R5	150, 250, 350
2	T7 - R6	150, 250, 350
3	T7 - R7	150, 250, 350
4	T13 - R7	150, 250, 350
5	T13 - R5	150, 250, 350
6	T13 - R6	150, 250, 350
7	T5 - R6	150, 250, 350
8	T5 - R7	150, 250, 350
9	T5 - R5	150, 250, 350

METHOD OF APPROACH

In order to determine the location and size of the crack, three different approaches were presented by students, which include: i) analyzing the ratio of the raw signals, ii) examining the ratio of scattered signal, and iii) evaluating the damage index obtained from the signals.

Method 1: Based on the Raw Signal Analysis

With this first method, the phase velocity and the time of arrival of the Lamb wave mode are initially calculated for different paths from the dispersion curves of the aluminum plate. Once the phase velocity and the time of arrival have been calculated, a signal region to analyze the data must be identified, which is done by determining a time window. Since each transmitter-receiver path has a time calculated from its corresponding phase velocity, this time is added with the time of the transmitter signal to obtain a total time window for overlaying on top of the receiver signal data. Based on the theoretical dispersion curves, A0 lamb waves have lower velocities and a slower time of arrival compared to S0 lamb waves, so the former is used as a starting point for obtaining the signal region of interest. By adding the A0 lamb wave's time of arrival with the time duration of the transmitter's tone-burst signal, it yields the total time window to obtain the signal region of interest. With the signal region determined, the signal ratio can now be computed by taking the mean difference between the baseline and damaged signal, as shown in Equation 1 and dividing it by the baseline signal, as shown below in Equation 2. Note that the damaged signal only includes data from the

region of the total time window calculated previously. The computed signal ratio is then used as a threshold for identifying if there is a crack along that transmitter-receiver path.

$$\text{Signal Difference} = (\text{Baseline Signal} - \text{Damaged Signal}) \tag{1}$$

$$\text{Signal Ratio} = \frac{\text{Mean}(|\text{Signal Difference}|)\ )}{\text{mean}(|\text{Baseline}|)} \tag{2}$$

Method 2: Based on the Scatter Signal Analysis

In this second method, the localization algorithm begins by identifying the S0 wave packet in the baseline and damage signals. The S0 wave packet is the first to arrive at the receiver. These two waveforms are then subtracted from each other to form a scatter signal. Once the scatter signal has been formed for all the paths, the maximum amplitude of the scatter signal for each path is recorded and ranked. A scatter wave with the maximum amplitude (A_s) is identified. Then the highest amplitude of the flawed or damage signal (A_f) are identified and recorded. The ratios of these amplitudes (α) are then computed as shown in Equation 3. Each path is denoted by using the subscript i = 1,2...9.

$$\alpha_i = \frac{A_s}{A_f} \tag{3}$$

The path length (L_i), from transmitter to receiver, is computed using the Equation 4 since the sensor locations are known.

$$L_i = \sqrt{(xT_i - xR_i)^2 + (yT_i - yR_i)^2} \tag{4}$$

The ratios α_i are then multiplied by their corresponding path lengths L_i and used to divide a unitarea of the surface. The result is a spacing (d_i) by which two parallel lines (top and bottom) are projected from both path lines that have been identified, which matches the intuition of a large scatter having parallel lines close to the path lines and vice versa. Mathematically, this is represented as shown in Equation 5 below:

$$d_i = \frac{\text{Unit Area}}{\alpha_i L_i} \tag{5}$$

Method 3: Based on the Damage Index

Within this last method, two approaches are used to calculate the size of the crack as well as the location of the crack. The size is determined using an energy-based damage index, and the location is determined with a scheme based on phase shift of the scatter signal compared to the baseline signal. To calculate the size of the crack, the following energy-based damage index was used [5]:

$$\mathrm{DI} = \left(\frac{\int_{t_{start}}^{t_{end}} (\mathrm{S0, scatter})^2 \, \mathrm{dt}}{\int_{t_{start}}^{t_{end}} (\mathrm{S0, baseline})^2 \, \mathrm{dt}} \right)^{0.5} \quad (6)$$

In the calculation of the DI, the envelope of the guided wave signal was used. The start of the S0 mode is defined as the first time where the smoothed sensor signal or the envelope rises above a predetermined value. The end is determined using the "findpeaks" function of MATLAB where the negative of the smoothed sensor data occurs for the baseline signal. The same timespan is then applied to the damaged and scatter signals. From the start and end times, the square of the smoothed function is used to calculate the damage index for each transmitter-receiver pair. The damage index essentially represents the fraction of total wave energy that is absorbed by damage in each path – this should, for cracks, then be correlated to length. Ihn et al performed this correlation of crack length to damage index in a 3.2 mm thick aluminum plate, making the assertion that as long as a crack is on or near the path of interest, there is a direct relationship between the crack length and the damage index.

$$\mathrm{DI} = 0.0464 \times \text{crack length} \quad (7)$$

Making the assumption that the crack is on the path with the highest damage index, the Equation 7 can then be applied to the highest damage index to determine an approximate crack length. DI calibration is required with a 2.1 mm thick plate to get more accurate results.

In order to determine the crack location, for each transmitter and receiver pair, the phase shift between the baseline S0 mode and the scattered S0 mode is calculated. The scattered S0 mode is caused by reflections from the crack. Using this information, it is possible to determine how far off the crack is from the direct path of the signal from the transmitter to the receiver. The peak detection scheme was used to determine the amount of shift, I_{shift}, which is the number of time intervals shifted from the baseline signal to the scatter. Using I_{shift}, the maximum possible distance of the crack from a signal path can be obtained from the following equations.

Note that x stands for the direct distance between the transmitter and receiver, and Δx stands for the additional distance traveled by the scatter signal compared to the baseline.

$$v_{s0} = 5000 \; m/s \quad (8)$$

$$\Delta T_{sactter} = \frac{I_{shift}}{fs} \quad (9)$$

$$\Delta x = v_{s0} \times \Delta T_{scatter} \quad (10)$$

$$y_{max} = \sqrt{\left(\frac{x + \Delta x}{2}\right)^2 + \left(\frac{x}{2}\right)^2} \quad (11)$$

By adding the length of crack to the crack location, we can calculate the bounds around each signal path that encompass the entirety of the crack. By finding the intersection of each of these bounds, the area of interest for the crack location can be narrowed down. Lastly, the centroid of the intersection can be calculated to provide a location estimate for the crack.

RESULTS AND DISCUSSIONS

Figure 2 shows the envelope of the ultrasonic signals and the portion of the S0 mode that were used to find the damage locations for path 8 and 350 kHz actuation center frequency. In Figure 3, the signal ratios were first computed for a crack with an unknown location. As shown in Figure 3, the signal ratios are presented in the table on the left, with the magnitudes indicated in the shades of red.

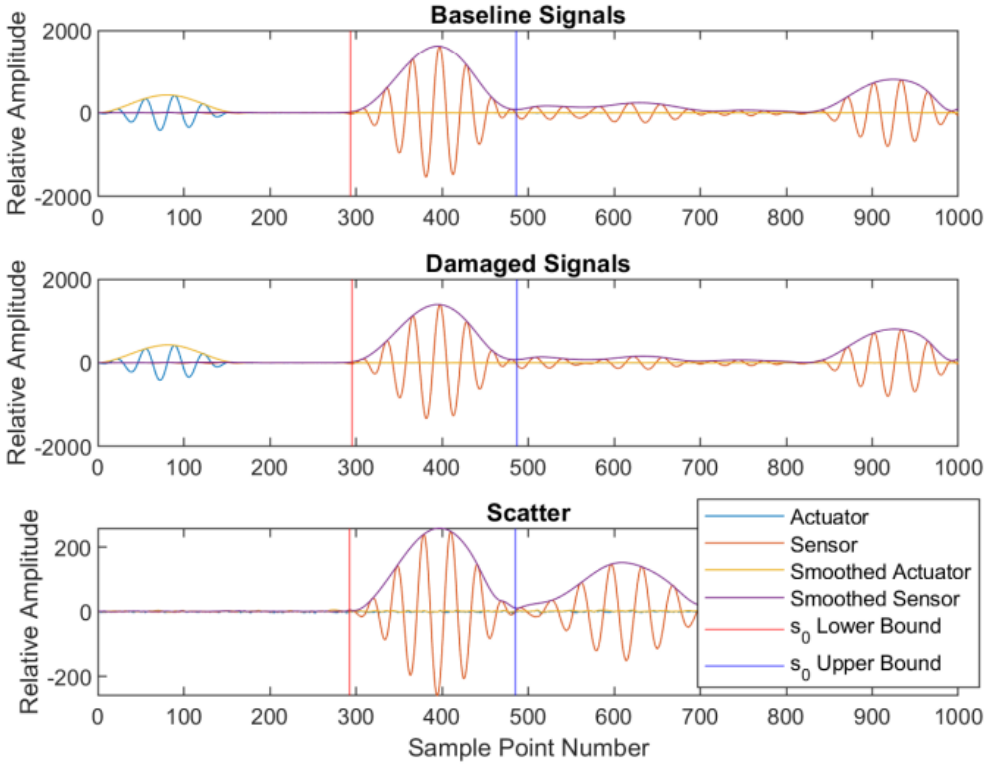

Figure 2. A representative signal with the envelope from path 8 for 350 kHz actuation frequency: the baseline signal, damage signal and the scatter signal are shown along with the lower bound and upper bound of the S0 mode.

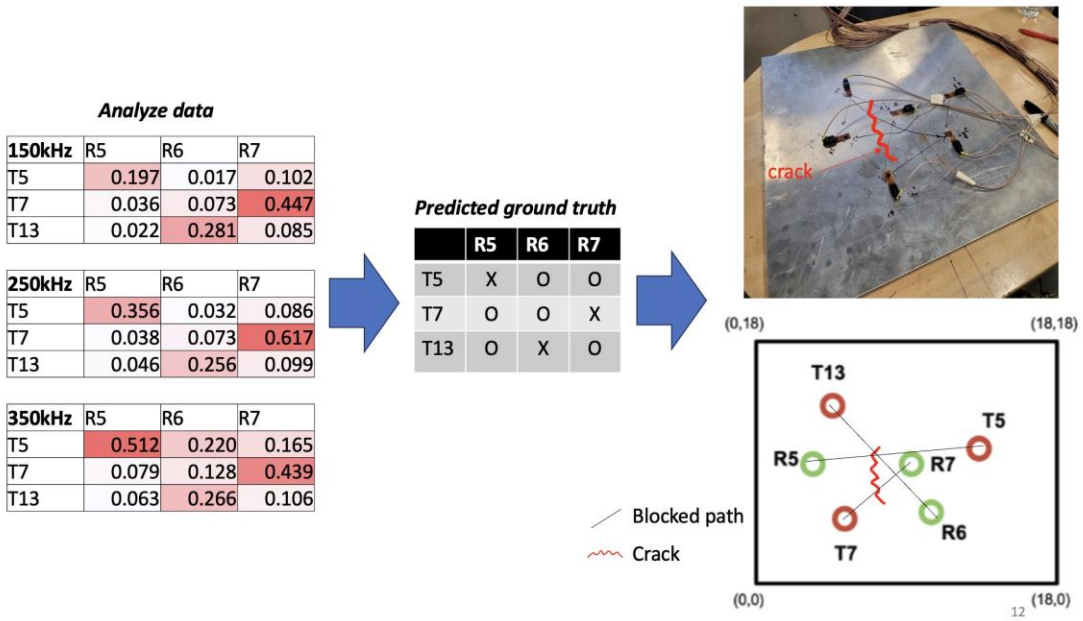

Figure 3. This figure shows the crack location prediction results using method 1; note that accurate crack prediction is obtained.

From the analyzed data, the paths of the blocked signals are deduced. For this specific case, the crack stretches from T13-R6, T5-R5, and T7-R7 paths and is shown on the right in Figure 3. By carefully analyzing the sensor data, the location of the crack was accurately determined, which is crucial for identifying potential damage in structures. The algorithm demonstrated sufficient accuracy for locating the crack when compared to the actual specimen, showcasing its potential and effectiveness in real-world applications.

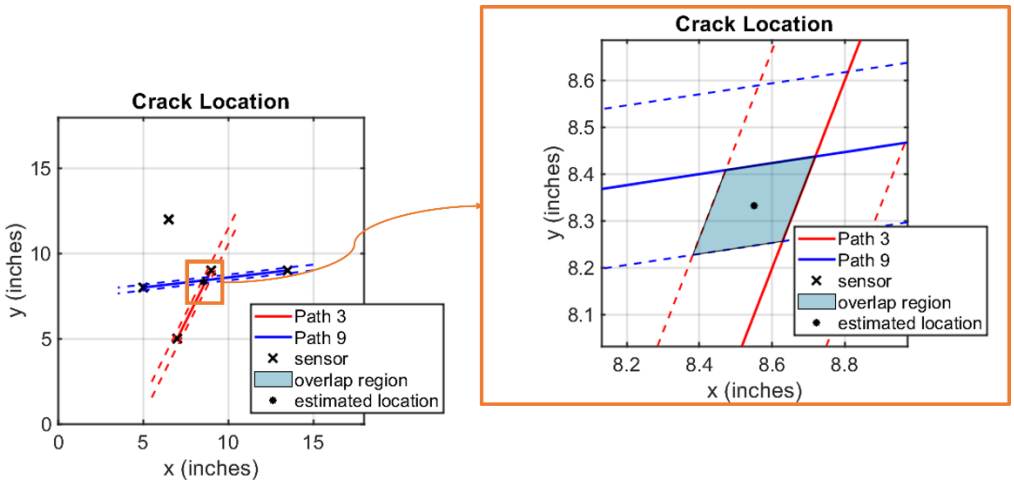

Figure 4. Determination of crack location by method 2: the location of the crack provided with this method coincides with the actual crack.

From Figure 4, it is shown that method 2 can achieve fairly accurate results for crack localization using PZT sensors. The area given by method 2 was accurate in providing a generalized location of the fault on the plate, with an estimated location ranging from 0.03 to 0.4 inches to the real fault location.

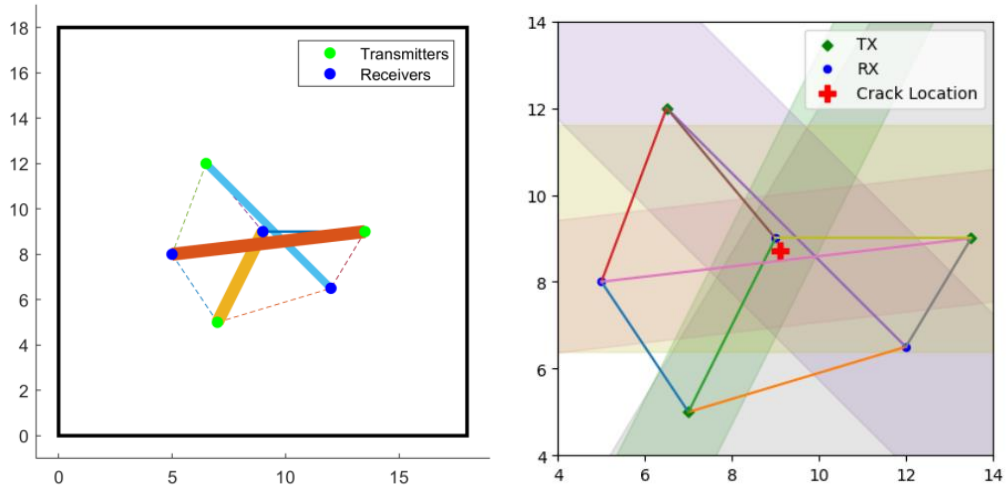

Figure 5: (left) Damage index for each transmitter-receiver pair caused by a crack: thicker lines denote higher damage index, dashed lines represent that the values are below damage threshold; (right) the location estimation of the crack by method 3.

The highest damage index of any signal path was 0.488, which was calculated from Equation 6. It is assumed that the signal path with the highest damage index intersected with the crack and this damage index correlated to a length of 10.5 mm. However, the length of the actual crack is 0.5 inch. The representation of damage indexes on each path is shown in Figure 5 (left). Using the location calculation method described in method 3, the crack location was determined to be around (9.06 in, 8.67 in). In the right image of Figure 5, the bounds around signal paths, as well as the localization at the intersection of all the bounds can be observed. The calculated crack location lies near signal paths with higher damage indices. This strengthens the validity of the proposed crack location estimate.

VALIDATION

Figure 6 shows the exact location of the crack with respect to the position of the sensors. It is to be mentioned here that the location of the crack was kept hidden during the analysis of the ultrasonic guided wave signal data. As a result, the location of the crack was found in a blind way just by analyzing the guided wave signal data. By observing the crack location from Figure 6, and comparing with Figure 3, 4 and 5, it can be concluded that the crack location was accurately identified with the three methods presented in this study.

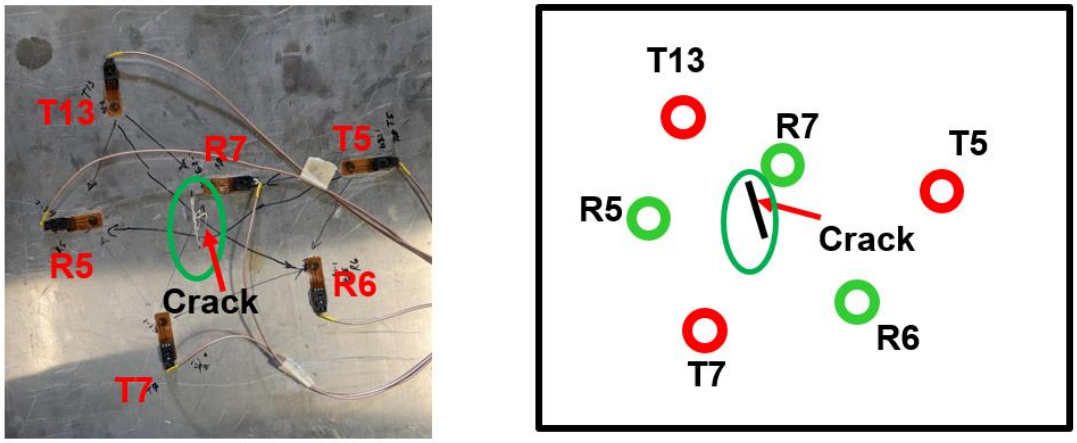

Figure 6: The exact location of the crack is shown here with respect to the position of the sensors.

Table 2: Accuracy and validation summary by method 2 and 3.

Flaw Type	**% Error in x-coordinate**	**% Error in y-coordinate**	**Distance between real and estimated flaw locations**
Patch-1	4.91	0.290	0.408 in
Patch-2	0.393	0.174	0.0292 in
Crack (method 2)	12.77	1.2	1.25
Crack (Method 3)	13.26	4.87	1.36

CONCLUSION

In this work, three different methods for localizing damage or crack in an aluminum plate using ultrasonic guided Lamb waves were investigated and assessed. Ultrasonic waves were transmitted and received by piezoelectric transducers for three different actuation frequencies at 150 kHz, 250 kHz and 350 kHz. In method 1, only the raw signals were used to localize damage. In method 2, instead of the raw signals, the scatter signals were utilized. In method 3, damage indices were obtained from the signals and utilized to provide location and size estimate of the damage. A bounding box for the location of the crack was also provided. In all three cases, only the S0 mode was utilized. It was shown that although the analysis method was fairly simple, it is possible to obtain an accurate estimate of the crack location based on the ultrasonic signals.

REFERENCES

1. Farrar, Charles R., and Keith Worden. "An introduction to structural health monitoring." *Philosophical Transactions of the Royal Society A: Mathematical, Physical and Engineering Sciences* 365.1851 (2007): 303-315.
2. Yadav, Susheel Kumar, et al. "Reliability of crack quantification via acousto-ultrasound active-sensing structural health monitoring using surface-mounted PZT actuators/sensors." *Structural Health Monitoring* 20.1 (2021): 219-239.
3. Balageas, Daniel, Claus-Peter Fritzen, and Alfredo Güemes, eds. *Structural health monitoring*. Vol. 90. John Wiley & Sons, 2010.
4. Chang, Fu-Kuo, et al. "Structural health monitoring." *System health management: with aerospace applications* (2011): 419-428.
5. Ihn, Jeong-Beom, and Fu-Kuo Chang. "Pitch-catch active sensing methods in structural health monitoring for aircraft structures." *Structural Health Monitoring* 7.1 (2008): 5-19.
6. Ihn, Jeong-Beom, and Fu-Kuo Chang. "Detection and monitoring of hidden fatigue crack growth using a built-in piezoelectric sensor/actuator network: I. Diagnostics." *Smart materials and structures* 13.3 (2004): 609.
7. Ihn, Jeong-Beom, Fu-Kuo Chang, and Holger Speckmann. "Built-in diagnostics for monitoring crack growth in aircraft structures." *Key engineering materials* 204 (2001): 299-308.
8. Farhangdoust, S., Tashakori, S., Baghalian, A., Mehrabi, A., & Tansel, I. N. (2019, March). Prediction of damage location in composite plates using artificial neural network modeling. In Sensors and Smart Structures Technologies for Civil, Mechanical, and Aerospace Systems 2019 (Vol. 10970, pp. 100-110). SPIE.
9. Giurgiutiu, Victor. *Structural health monitoring: with piezoelectric wafer active sensors*. Elsevier, 2007.
10. https://www.acellent.com/